

ATLAS Sensitivity to the Flavour-Changing Neutral Current Decay $t \rightarrow Zq$

Leila Chikovani

Institute of Physics of the Georgian Academy of Sciences,

Tamar Djobava

High Energy Physics Institute, Tbilisi State University,

ABSTRACT

The sensitivity of the ATLAS experiment to the top-quark rare decay via flavor-changing neutral currents $t \rightarrow Zq$ (q represents c and u quarks) has been studied at $\sqrt{s}=14$ TeV in two decay modes:

1. The pure leptonic decay of gauge bosons: $t\bar{t} \rightarrow ZqWb \rightarrow l^+l^-jl^\pm\nu b$, ($l=e, \mu$).
2. The leptonic decay of Z bosons and hadronic decay of W bosons: $t\bar{t} \rightarrow ZqWb \rightarrow l^+l^-jjjb$, ($l=e, \mu$).

The dominant backgrounds $Z + jets$, WZ and $t\bar{t}$ have been analysed. The signal and backgrounds were generated via PYTHIA 5.7, and simulated and analysed using ATLFast 2.14. A branching ratio for $t \rightarrow Zq$ as low as 2.0×10^{-4} for the leptonic mode and 5.9×10^{-4} for hadronic mode could be discovered at the 5σ level with an integrated luminosity of 100 fb^{-1} .

1 Introduction

The existence of the top quark has been established at the Fermilab Tevatron by the CDF and DO Collaborations [1]. Due to the large value of the top quark mass, of order the Fermi scale, the top quark couples strongly to the electroweak symmetry breaking sector. If anomalous top quark couplings beyond the Standard Model (SM) exist, they could affect top quark production and decay processes at hadron and $e^+ e^-$ colliders [2,3]. For example, study of the flavour-changing neutral current top quark decay $t \rightarrow Zq$ (where q represents either c or u quarks) is of great interest. As is well known [4,5], the LHC can be considered as a “top factory”, producing about 80,000 $t\bar{t}$ events per day at $L = 10^{33} \text{ cm}^{-2} \text{ s}^{-1}$, making the LHC an ideal place to explore this rare decay.

In this note, we present a study of the sensitivity of the ATLAS experiment to the branching ratio of the top-quark rare decay mode $t \rightarrow Zq$ ($q = u, c$). In the framework of the Standard Model, the loop suppression and heaviness of gauge bosons make this process extremely rare. The SM prediction for the branching ratio, of order 10^{-13} [6], would render the decay unobservable even with the large samples of top quarks expected at the LHC. However, other models predict significantly larger branching ratios for this process. For example, in two-Higgs-doublet models, the value of $\text{Br}(t \rightarrow Zq)$ can reach $\sim 10^{-9}$ [7], while Supersymmetric (SUSY) models (without R -parity) can have even much higher values, $\text{Br}(t \rightarrow Zq) \sim 10^{-4}$ [8].

Experimentally, little is known about this decay. The only existing limit comes from a CDF analysis of its Run1 data [9], yielding $\text{Br}(t \rightarrow Zq) < 33\%$ (95% CL). Given the SM prediction, an observation of this decay mode, even at the LHC, would provide a clear signal of new physics beyond the SM, such as new dynamical interactions of top quark, multi-Higgs doublets, exotic fermions or other possibilities [5,6,7]. In addition, this mode is of interest since, if the branching ratio were large, events of the form $t\bar{t} \rightarrow ZZ + cc$ could prove to be a serious background to events containing Z boson pairs and jets from cascade decays of squarks and gluinos [10].

The dominant mechanism for top quark production at the LHC is $t\bar{t}$ pair production via $gg, q\bar{q} \rightarrow t\bar{t}$. The analyses presented here focus on two different final state topologies of $t\bar{t} \rightarrow ZqWb$:

1. The purely leptonic decay of both gauge bosons:

$$t \rightarrow Zq \rightarrow l^+ l^- j, \bar{t} \rightarrow Wb \rightarrow l^\pm \nu b \text{ (l=e, } \mu\text{)}$$

2. The leptonic decay of the Z boson and hadronic decay of the W boson:

$$t \rightarrow Zq \rightarrow l^+ l^- j, \bar{t} \rightarrow Wb \rightarrow jjb \text{ (l=e, } \mu\text{)}$$

The value of the branching ratio of the second (“hadronic”) mode is three times higher than for the first (“leptonic”) one. However, the hadronic mode suffers from enormous QCD-backgrounds, while the leptonic mode has a very distinct experimental signature. Both modes have been studied, and the results of each analysis will be presented below.

2 Monte Carlo Event Generation

The dominant source of top quark production at the LHC is pair-production via $gg, q\bar{q} \rightarrow t\bar{t}$. PYTHIA 5.7 was set up to produce $t\bar{t}$ events at $\sqrt{s} = 14$ TeV and $m_{top} = 174$ GeV, with proton structure functions CTEQ2L. Initial and final state QED and QCD (ISR, FSR) radiation, multiple interactions, fragmentations and decays of unstabled particles were enabled.

The decay $t \rightarrow Zq$ is not implemented in the standard release of PYTHIA. To include this process in PYTHIA, all individual decay channels of the top quark were first switched off, except for $t \rightarrow Wb$ and $t \rightarrow Ws$. The channel $t \rightarrow Ws$ was then replaced by the decay $t \rightarrow Zq$, by replacing W by Z and s by $c(u)$. The total cross-section for $t\bar{t}$ production was assumed to be $\sigma_{t\bar{t}}=800$ pb [12].

The analyses reconstructed the Z boson via its leptonic decay, $Z \rightarrow l^+l^-$. The experimental signature included, therefore, a pair of isolated charged leptons, as well as several jets. The SM backgrounds considered for this process were $Z + jets$ production, WZ production, and $t\bar{t} \rightarrow WbWb$ production.

$Z + jets$ production at the LHC has a relatively large cross-section, dominated by $gg \rightarrow Zq$ and $q\bar{q} \rightarrow Zg$ processes. To decrease the size of the background sample which needed to be generated, thresholds were imposed at the generator level on the invariant mass, $\hat{m} = \sqrt{\hat{s}} > 130$ GeV, and transverse momentum, $\hat{p}_\perp > 50$ GeV, of the hard scattering process. The cross-section for this subsample of events was $\sigma_{Z+jets}=3186$ pb.

The WZ background is the electroweak process $pp \rightarrow W^\pm Z + X$, and has an assumed cross-section of $\sigma_{WZ} = 26.58$ pb.

The performance of the ATLAS detector was simulated using the fast simulation package ATLFast 2.14 [11], which uses parametrizations of the detector resolution functions.

3 The Leptonic Decay Mode

The final state for the leptonic decay mode is $t\bar{t} \rightarrow ZqWb \rightarrow l^+l^- j l \nu b$. The experimental signature therefore includes three isolated charged leptons, two of which reconstruct a Z boson, and large missing transverse energy due to the neutrino.

The backgrounds considered were $Z+jets$ production, followed by the decay $Z \rightarrow l^+l^-$, $pp \rightarrow W^\pm Z + X \rightarrow l^\pm \nu l^+ l^- + X$, and $t\bar{t} \rightarrow W^+ b W^- \tilde{b} \rightarrow l^+ \nu b l^- \tilde{\nu} b$. Background samples of $2.1 \times 10^7 Z + jets$ events, 35700 WZ events, and $3.7 \times 10^6 t\bar{t}$ events were generated. Assuming the production cross-sections given earlier, and including the relevant branching ratios, these background samples correspond to an integrated luminosity of 100 fb^{-1} .

Table 1 summarizes the effects of the sequential application of the various analysis cuts on the background samples and on the sample of 20565 signal events of the topology $t\bar{t} \rightarrow ZqWb \rightarrow l^+ l^- j l \nu b$.

Description of Cuts	$t \rightarrow Zc$		Background Processes					
	Signal		Z+jets		Z+W		$t\bar{t}$	
	Nevt	Eff (%)	Nevt	Eff (%)	Nevt	Eff (%)	Nevt	Eff (%)
Nevt gen.	20565		$2.1 \cdot 10^7$		35000		$3.7 \cdot 10^6$	
Preselection	16497	80.2	$3.7 \cdot 10^5$	1.7	2941	8.2	$8.5 \cdot 10^5$	29.4
3 leptons	8885	43.3	945	$4.4 \cdot 10^{-3}$	1778	5.0	1858	$5.0 \cdot 10^{-2}$
$p_T > 30 \text{ GeV}$	6730	32.7	80	$3.7 \cdot 10^{-4}$	1252	3.5	1600	$4.3 \cdot 10^{-2}$
2 jets	4063	19.8	31	$1.5 \cdot 10^{-4}$	225	0.6	596	$1.6 \cdot 10^{-2}$
$M_Z \pm 6 \text{ GeV}$	3450	16.8	24	$1.1 \cdot 10^{-4}$	180	0.5	29	$7.8 \cdot 10^{-4}$
one b -tag	1678	8.2	10	$4.7 \cdot 10^{-5}$	28	0.04	10	$2.7 \cdot 10^{-4}$
$M_t \pm 8 \text{ GeV}$	728	3.5	0	0	1	$2.8 \cdot 10^{-3}$	3	$8.1 \cdot 10^{-5}$
$M_t \pm 12 \text{ GeV}$	973	4.7	0	0	1	$2.8 \cdot 10^{-3}$	4	$1.1 \cdot 10^{-4}$
$M_t \pm 24 \text{ GeV}$	1264	6.1	0	0	2	$5.6 \cdot 10^{-3}$	5	$1.3 \cdot 10^{-4}$

Table 1: The numbers of events and efficiencies (%) of kinematic cuts applied in sequence for the signal and backgrounds for the leptonic mode. The numbers do not include the lepton identification efficiencies.

Preselection cuts were first applied, requiring the presence of at least three charged leptons (electrons with $p_T > 5 \text{ GeV}$ and muons with $p_T > 6 \text{ GeV}$) within pseudorapidity $|\eta| < 2.5$. Of these, at least one pair of leptons must be of opposite sign and same flavour, compatible with them being produced from a Z decay. In addition, the number of jets in the event with $p_T^{jet} > 15 \text{ GeV}$ was required to be at least two. The requirement of three leptons reduces significantly the $Z + jets$ and $t\bar{t}$ backgrounds, while the requirement of two jets reduces significantly WZ and $Z + jets$ backgrounds.

The lepton criteria were then tightened, by requiring the presence of at least three isolated, charged leptons (electrons or muons) with $p_T^l > 20 \text{ GeV}$ and $|\eta^l| < 2.5$. The isolation criterion required that there be no additional track with $p_T > 2 \text{ GeV}$ in a cone

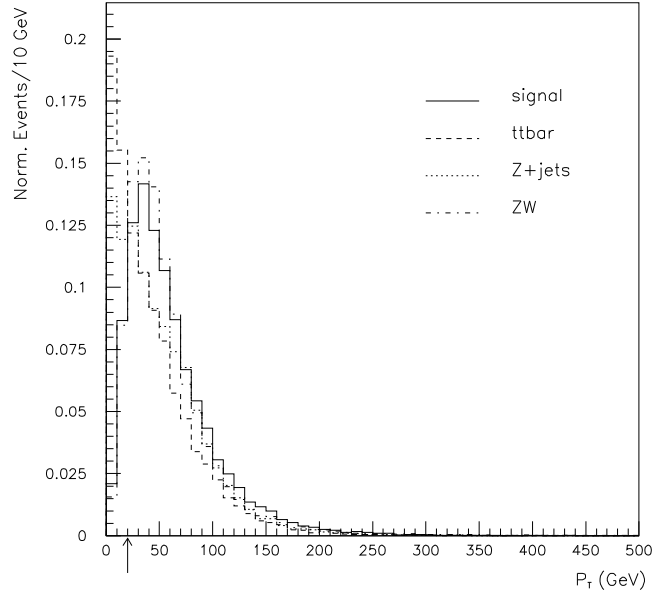


Figure 1: The p_T distributions of leptons which give a dilepton invariant mass within the accepted window around the Z mass, for leptonic mode signal and backgrounds, normalised to unity. The arrow indicates the threshold value p_T^l used for the analysis cut.

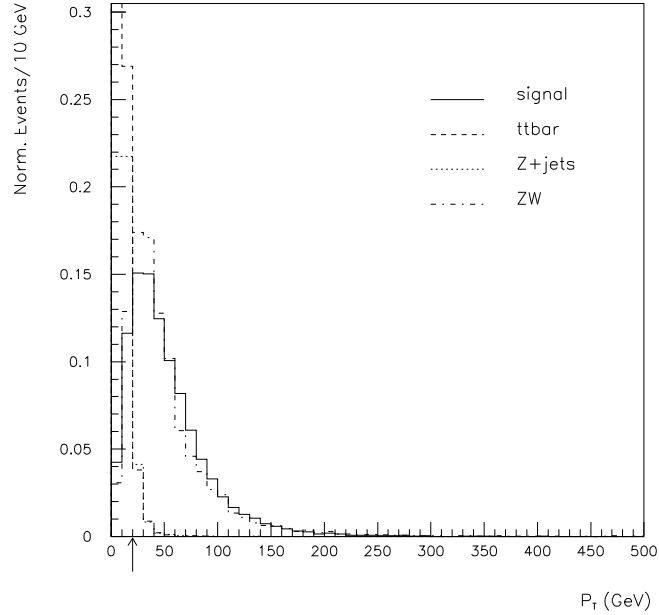


Figure 2: The p_T distribution of the third lepton for the leptonic mode signal and backgrounds, normalised to unity. The arrow indicates the threshold value p_T^l used for the analysis cut.

of $\Delta R = \sqrt{(\Delta\phi)^2 + (\Delta\eta)^2} = 0.3$ around the lepton direction. Fig. 1 presents the p_T distribution of the two leptons consistent with originating from a Z decay for signal and backgrounds, while Fig. 2 shows the p_T distribution for the third lepton. Tightening the lepton criteria significantly reduces the $Z + jets$ and $t\bar{t}$ backgrounds, where any third lepton found typically comes from cascade decays of b -jets.

The next requirement, namely that the missing transverse momentum in the event satisfies $p_T^{miss} > 30$ GeV, is effective at further reducing the $Z + jets$ background (see Fig. 3), while having little impact on the signal and other background sources.

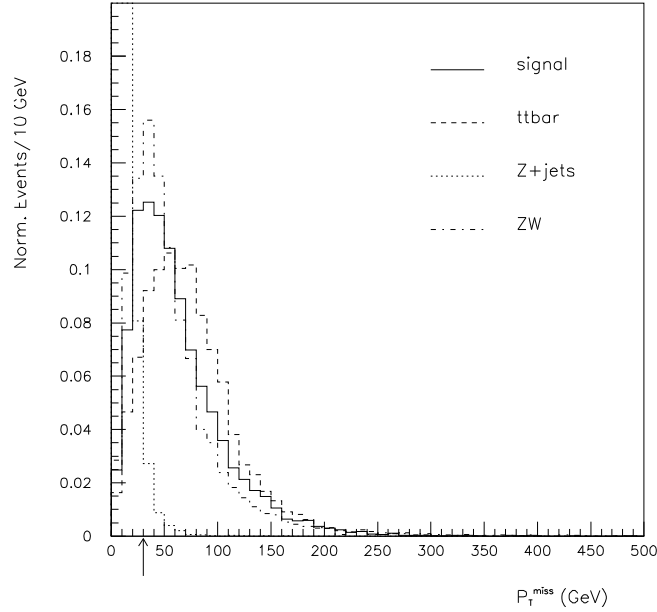


Figure 3: The reconstructed p_T^{miss} distributions for leptonic mode signal and backgrounds, normalised to unity. The arrow indicates the threshold value used for the kinematic cut.

Next, it was demanded that there be at least two jets with $p_T^{jet} > 50$ GeV, $|\eta^{jet}| < 2.5$, and satisfying the following isolation conditions: $\Delta R_{jj} > 0.4$ (jet-jet isolation) and $\Delta R_{lj} > 0.4$ (lepton-jet isolation). Fig. 4 presents the number of jets with $p_T^{jet} > 50$ GeV in an event. One can see that the cut requiring the presence of two and more such jets in each event effectively suppresses the WZ background.

The presence of a reconstructed $Z \rightarrow l^+l^-$ decay is a powerful cut against the $t\bar{t}$ background. A like-sign, same-flavor pair of isolated leptons was required to reconstruct to the Z mass within a window of $M_Z \pm 6$ GeV mass window. Fig. 5(a) presents the distribution of reconstructed invariant mass of ll pairs m_{ll} , for all dilepton combinations for the signal events. The width of the accepted window corresponds to approximately

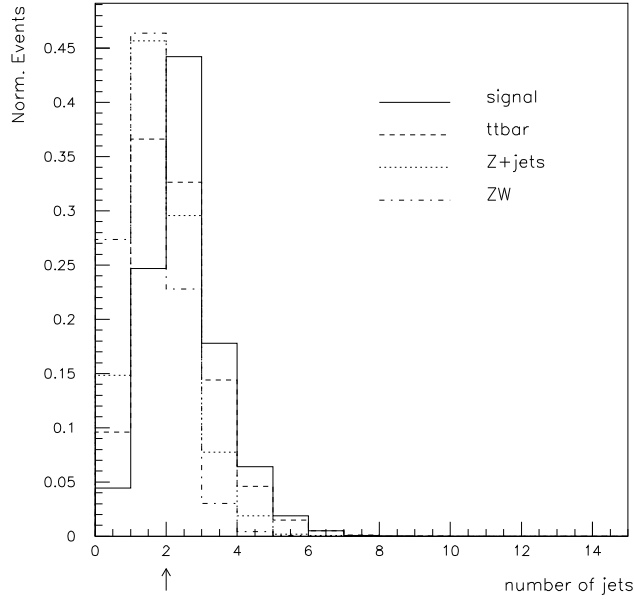


Figure 4: Distribution of jet multiplicity (threshold at $p_T^{jet} > 50$ GeV) for signal and backgrounds, normalised to unity. The arrow indicates the threshold value of the number of jets used for the kinematic cut.

twice the Z mass resolution of about 2.9 GeV.

The next requirement was the presence in the event of one tagged b -jet, which is effective at further reducing the WZ background (see Fig. 6).

Finally, a peak at the top quark mass in the Zj invariant mass distribution was sought. In Fig. 5(b), the distribution of reconstructed invariant mass m_{lj} for all combinations of llj is presented for the signal events. The top quark mass resolution is $\sigma(m_{lj}) = 14$ GeV. Accepted combinations were required to lie within a window around the known top quark mass. As a check of the stability of the results, three different mass window were considered: $m_{Zj} = m_t \pm 8$ GeV (narrow cut), $m_t \pm 12$ GeV ($\sim \sigma$), and $m_t \pm 24$ GeV ($\sim 2\sigma$). The top mass window removes almost completely the remaining background.

As summarized in Table 1, the final signal efficiency was 6.1% for the $m_t \pm 24$ GeV mass window, with a total background of 7 events for an integrated luminosity of 100 fb^{-1} . The results in the table do not yet include the lepton identification efficiencies. Assuming an efficiency of 90% for each of the three leptons, the results correspond to a 5σ discovery potential for $\text{Br}(t \rightarrow Zq)$ as low as 2.0×10^{-4} and for an integrated luminosity of 100 fb^{-1} . This result is in good agreement with that of reference [13].

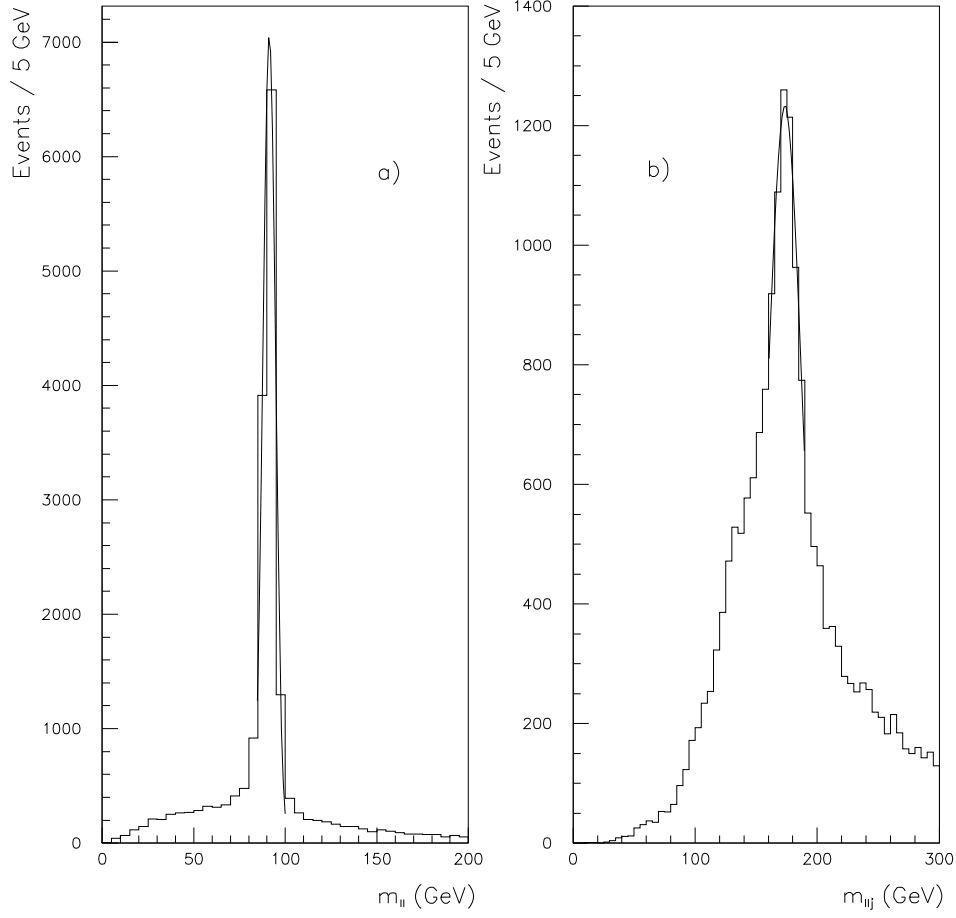


Figure 5: (a) Distribution of reconstructed invariant mass of the lepton pairs, m_{ll} for the leptonic mode. (b) Distribution of reconstructed invariant mass of $t \rightarrow Zq \rightarrow llj$ for the leptonic mode.

4 The Hadronic Decay Mode

The final state for the hadronic W decay mode is $t\bar{t} \rightarrow ZcWb \rightarrow l^+l^-jjjb$. The experimental signature for the hadronic mode includes, therefore, two isolated charged leptons which originate from the Z decay, and four energetic jets.

This mode has the following backgrounds: $Z(\rightarrow ll) + jets$, $pp \rightarrow W^\pm Z + X \rightarrow jjl^+l^- + X$, and $t\bar{t} \rightarrow WbWb$ with the final state topologies (a) $l^+\nu bl^-\bar{\nu}b$, (b) $jbjbjb$, or (c) $l^+\nu bjjb$. In the case of (a), the additional two jets must come from QCD radiation, while in (b) and (c) the source of leptons is from cascade decays. Therefore, requiring

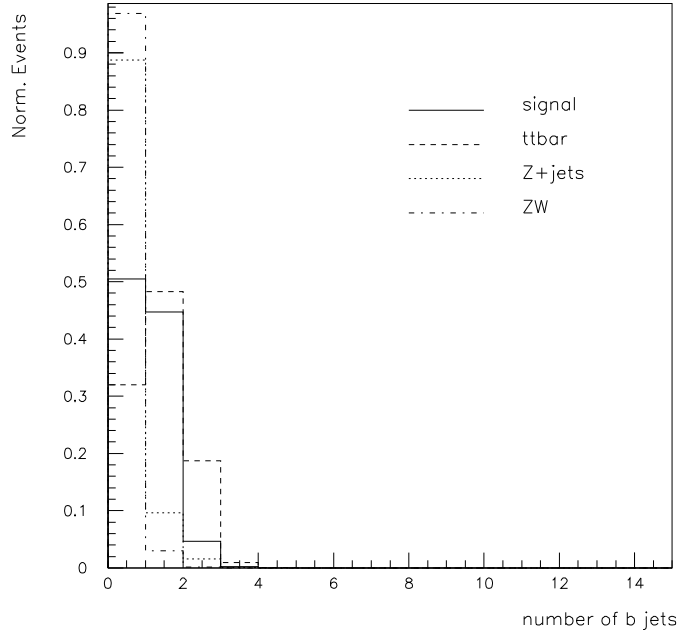


Figure 6: Distribution of b -jet multiplicity (threshold at $P_T^{jet} > 50$ GeV) for signal and backgrounds, normalised to unity.

two isolated energetic leptons and four energetic jets, among which only one is tagged as a b -jet, significantly suppresses the $t\bar{t}$ background. It has been checked that the small remaining $t\bar{t}$ background is removed by the reconstruction cuts asking for m_{ll} and m_{llj} to lie within windows around m_Z and m_t respectively. Therefore, the $t\bar{t}$ background is reduced to a negligible level, and is not considered further.

Background samples of $2.1 \times 10^7 Z + jets$ events, and $1.2 \times 10^5 WZ$ events were generated. Assuming the production cross-sections given earlier, and including the relevant branching ratios, these background samples correspond to an integrated luminosity of 100 fb^{-1} .

Table 2 summarizes the effects of the sequential application of the various analysis cuts on the background samples and on the sample of 19000 signal events of the topology $t\bar{t} \rightarrow ZqWb \rightarrow l^+l^-jjb$.

The analysis began with preselection cuts requiring that the event contains at least two charged leptons (electrons with $p_T > 5$ GeV within pseudorapidity $|\eta| < 2.5$ and muons with $P_T > 6$ GeV within pseudorapidity $|\eta| < 2.4$), and include a pair of opposite-sign and same-flavour leptons, compatible with them having come from a Z decay. In addition, the number of jets with $p_T^{jet} > 15$ GeV was required to be at least four. After preselection cuts, 46% of the signal events are accepted, while only 3.5% and 4.1% of the

$Z + jets$ and WZ background events, respectively, are retained.

The next cuts required the presence of two isolated leptons with $p_T^l > 20$ GeV and $|\eta^l| < 2.5$, and the demand for at least four jets with $P_T^{jet} > 50$ GeV and $|\eta^j| < 2.5$. Jet-jet and lepton-jet isolation criteria were then applied, as was done in the leptonic mode analysis.

A cut was then placed on the dilepton invariant mass, requiring that it lie within a window of ± 6 GeV around m_Z , the same mass window as used for the leptonic mode. Fig. 7(a) presents the distribution of reconstructed dilepton invariant mass for the signal sample.

To suppress the large remaining $Z + jets$ background, it was necessary to use the information that signal events contain, in addition to the decay $t \rightarrow Zq$, a hadronic decay $t \rightarrow Wb \rightarrow jjb$ of the other top quark. The hadronic top quark decay was, therefore, reconstructed as part of the signal requirement. First, a pair of jets was required to have an invariant mass m_{jj} with a window of ± 16 GeV around m_W . Fig. 8.a shows the distribution of reconstructed m_{jj} for the best combinations of jj for the signal events. The W mass resolution is $\sigma_{m_{jj}} = 8$ GeV.

The requirement was then made to have one jet tagged as a b -jet. Finally, the jjb invariant mass was required to lie within a window of ± 8 GeV around m_t . Fig. 8(b) presents the distribution of the reconstructed invariant top mass (m_{jjb}) for the best combinations of jjb for the signal. The top mass resolution is $\sigma(m_{jjb}) = 18.5$ GeV, implying that the mass window applied is rather narrow in order to get a large background rejection. The sequence of cuts required to reconstruct the hadronic decay of the other top quark dramatically suppresses the background, but also reduces the signal efficiency by almost an order of magnitude.

In Fig. 7.b the distribution of reconstructed $t \rightarrow Zq$ invariant top mass m_{llj} for the best combinations of llj is presented for the signal. The resolution σ of m_{llj} distribution is $\sigma_{m_{llj}} = 9.9$ GeV. For the reconstruction of the top mass for the decay $t \rightarrow Zq$, the same mass windows have been chosen as for the leptonic mode: $m_{Zq} \pm 8$ GeV (narrow cut), $m_{Zq} \pm 12$ GeV ($\sim \sigma$) $m_{Zq} \pm 24$ GeV ($\sim 2\sigma$).

It is worth mentioning that, in the mass window $m_{Zq} \pm 8$ GeV, 91% of the accepted events contain c -jets, $t \rightarrow llc$ and only 10% of events are reconstructed with light jets. By widening the mass window, the mixture of events reconstructed with light jets increases from 10% to 22%, but the number of events reconstructed with c -jets increases too.

The analysis cuts reduce the WZ background to a negligible level in three Zj mass windows. The $Z + jets$ background vanishes in mass window $m_{Zq} \pm 8$ GeV, while one event is accepted in $m_{Zq} \pm 12$ GeV, and two events in $m_{Zq} \pm 24$ GeV.

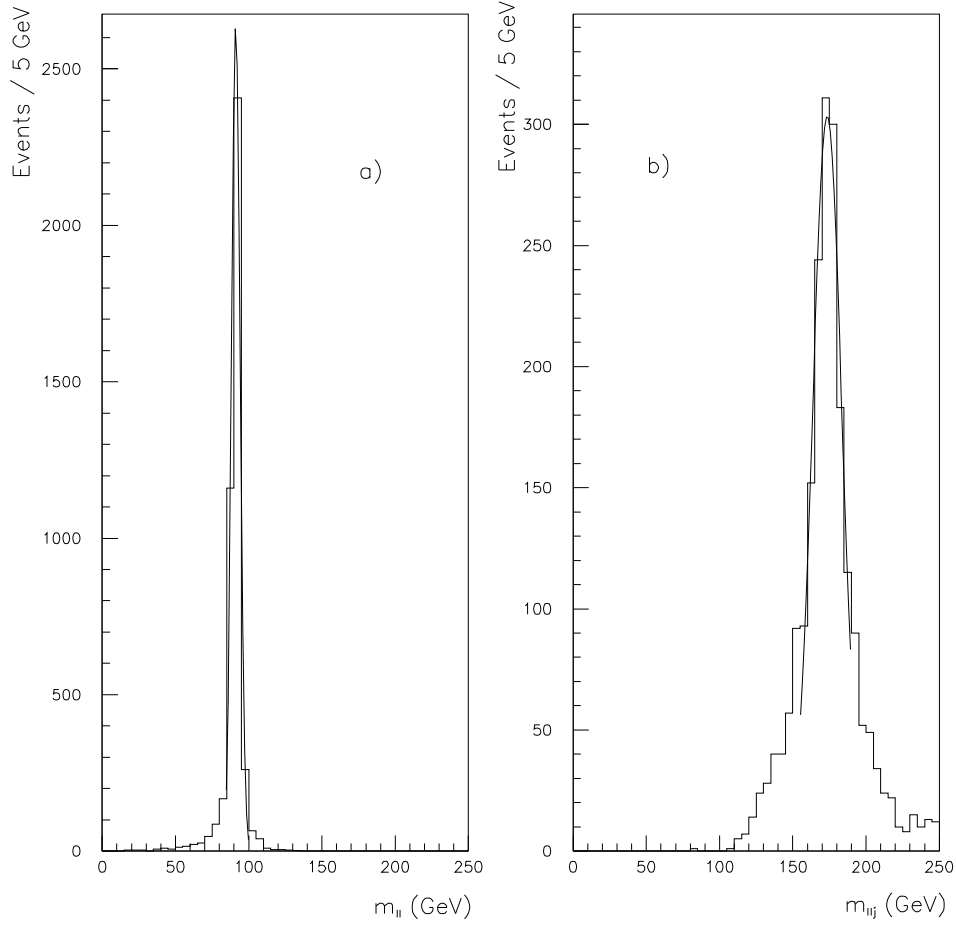


Figure 7: a) Distribution of reconstructed invariant mass of the lepton pairs, m_{ll} for the best combination (hadronic mode). b) Distribution of reconstructed invariant mass of $t \rightarrow llj$ for the best combination of llj (hadronic mode).

The results in Table 2 imply that a value of $\text{Br}(t \rightarrow Zq)$ as low as 5.9×10^{-4} could be discovered at the 5σ level with an integrated luminosity 100 fb^{-1} .

5 Conclusions

We have studied the ATLAS sensitivity to the FCNC top quark rare decay $t \rightarrow Zq$ ($q = u, c$) for an integrated luminosity of 100 fb^{-1} .

As summarized in Table 3, the results demonstrate that, in the leptonic mode, a branching ratio as low as 2.0×10^{-4} and, in the hadronic mode, as low as 5.9×10^{-4} could

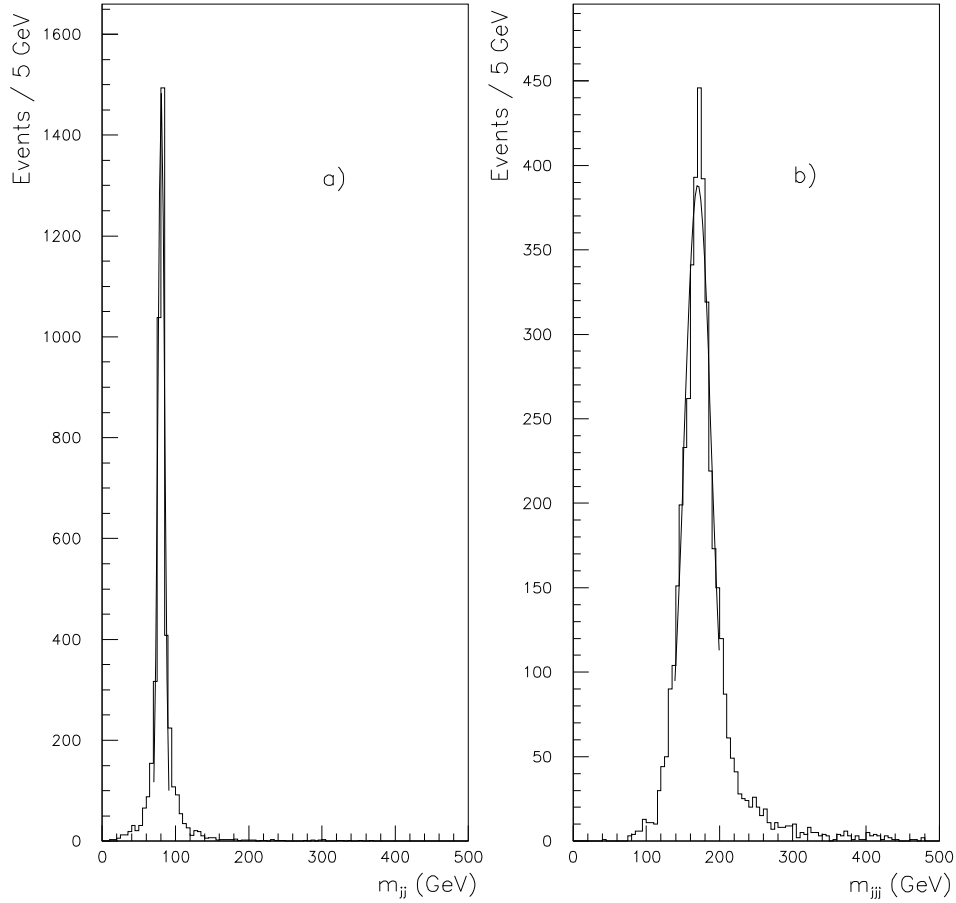


Figure 8: a) Distribution of reconstructed invariant mass of the jet pairs, m_{jj} for the best combination (hadronic mode). b) Distribution of reconstructed invariant mass of $t \rightarrow jjb$ for the best combination of jjb (hadronic mode).

be discovered at the 5σ level with an integrated luminosity of 100 fb^{-1} .

Table 4 compares the relative efficiencies of some of the important kinematic cuts for leptonic and hadronic modes of the signal. One can see that the relative efficiencies of leptons, jets, Z mass, b -jet and top mass cuts for leptonic and hadronic modes are in good agreement, as expected. This agreement supports the consistency of the two analyses, despite different versions of the ATLFAST code being used in the two cases.

Combining the results from the two decay modes extends the 5σ discovery potential down to a branching ratio as low as 1.8×10^{-4} .

Description of Cuts	$t \rightarrow Zc$ Signal		Background Processes			
			Z+jets		Z+W	
	Nevt	Eff (%)	Nevt	Eff (%)	Nevt	Eff (%)
Nevt gen.	19002		$2.1 \cdot 10^7$		$1.2 \cdot 10^5$	
Preselection	8742	46.0	$7.5 \cdot 10^5$	3.5	4970	4.1
2 leptons	7174	37.7	$5.9 \cdot 10^5$	2.8	4456	3.7
4 jets	2896	15.2	63478	0.29	400	0.3
$\Delta R_{jj} > 0.4$	2828	14.9	60421	0.28	390	0.3
$\Delta R_{lj} > 0.4$	2826	14.9	60394	0.28	361	0.3
$M_Z \pm 6 \text{ GeV}$	2426	12.8	50973	0.24	268	0.2
$M_W \pm 16 \text{ GeV}$	1006	5.3	14170	$6.6 \cdot 10^{-2}$	139	0.1
one b -tag	432	2.2	1379	$6.4 \cdot 10^{-3}$	11	$9.1 \cdot 10^{-3}$
$M_{Wb} = M_t \pm 8 \text{ GeV}$	106	0.6	90	$4.2 \cdot 10^{-4}$	1	$8.3 \cdot 10^{-4}$
$M_{Zq} = M_t \pm 8 \text{ GeV}$	46	0.2	0	0	0	0
$M_{Zq} = M_t \pm 12 \text{ GeV}$	58	0.3	1	$4.8 \cdot 10^{-6}$	0	0
$M_{Zq} = M_t \pm 24 \text{ GeV}$	74	0.4	2	$9.3 \cdot 10^{-6}$	0	0

Table 2: The numbers of events and efficiencies (%) of selection cuts applied in sequence for the signal in the hadronic decay mode.

Window for M_{Zq}	Sensitivity to $\text{Br}(t \rightarrow Zq)$		
	Leptonic Mode	Hadronic Mode	Combined Result
$M_t \pm 8 \text{ GeV}$	$2.80 \cdot 10^{-4}$	$9.60 \cdot 10^{-4}$	$2.60 \cdot 10^{-4}$
$M_t \pm 12 \text{ GeV}$	$2.34 \cdot 10^{-4}$	$6.70 \cdot 10^{-4}$	$2.18 \cdot 10^{-4}$
$M_t \pm 24 \text{ GeV}$	$2.01 \cdot 10^{-4}$	$5.86 \cdot 10^{-4}$	$1.80 \cdot 10^{-4}$

Table 3: Summary of the results.

Acknowledgements

We are very indebted to D.Froudevaux, J.Parsons, M.Cobal, E.Richter-Wass, S.Slabospitsky for very interesting and important discussions. We are very grateful to R.Mehdiyev for valuable advice. We would like to thank P.Jenni and T.Grigalashvili for their continuous support and encouragement during our work, and J.Khubua for providing the opportunity to proceed with this work in the future. The authors wish to thank Z.Menteshashvili for help during the preparation of the article.

C U T S	LEPTONIC MODE	HADRONIC MODE
	Rel.Effic. (%)	Rel.Effic. (%)
3l with $P_T^l > 20 \text{ GeV}$ in $ \eta^l < 2.5$	70.1	
2l with $P_T^l > 20 \text{ GeV}$ in $ \eta^l < 2.5$		82.0
2 isolated jets with $P_T^{jet} > 50 \text{ GeV}$	48.6	
4 isolated jets with $P_T^{jet} > 50 \text{ GeV}$		39.4
Lepton-jets isolation: $\Delta R_{lj} > 0.4$	94.0	99.0
Z mass $M_Z \pm 6 \text{ GeV}$	84.9	85.8
one tagged b jet in the event	48.6	42.9
$t \rightarrow Zq$ mass : $M_{Zq} \pm 8 \text{ GeV}$	43.4	43.4
$t \rightarrow Zq$ mass : $M_{Zq} \pm 12 \text{ GeV}$	49.2	54.7
$t \rightarrow Zq$ mass : $M_{Zq} \pm 24 \text{ GeV}$	75.3	69.8

Table 4: The relative efficiencies (%) of some of the kinematic cuts for leptonic and hadronic modes of the signal.

References

- [1] F.Abe et al. (CDF Collaboration), Phys.Rev.Lett. 74 (1995) 2626; S.Abachi et al. (DO Collaboration), Phys.Rev.Lett. 74 (1995) 2632
- [2] D.Carlson, E.Malkawi, and C.Yuan, Phys.Lett B337 (1994) 145; and references therein
- [3] D.Atwood, A.Kagan, and T.Rizzo, SLAC-PUB-6580 (hep-ph/9407408) and references therein
- [4] H.Fritzsh, Phys.Lett. B224 (1989) 423
- [5] T.Han, R.Peccei and X.Zhang, Nucl.Phys. B454 (1995) 527
- [6] B.Grzadkowski, J.Gunion and P.Krawczyk, Phys.Lett. B268 (1991) 106;
M.Luke and M.Savage, Phys.Lett. B307 (1993) 387;
G.Couture, C.Hamzaoui and M. Konig, Phys. Rev. D52 (1995) 1713
- [7] G.Eilam, J.Hawett and A.Soni, Phys.Rev. D44 (1991) 1473
- [8] C.S.Li, R.Oakes and J.M.Yang, Phys.Rev. D49 (1994) 293;
G.de Divitiis, R.Petronzio and L.Silvestrini, Nucl.Phys. B504 (1997) 45;
G.Couture, M.Frank and H.König, Phys.Rev. D56 (1997) 4213

- [9] F.Abe et al. (CDF Collaboration), Phys.Rev.Lett. 80 (1998) 2525
- [10] ATLAS Collaboration, Technical Proposal, CERN/LHCC/94-43, 1994
- [11] E.Richter-Was, D.Froidevaux and L.Poggioli, ATLAS Internal Note ATL-PHYS-98-131, 1998
- [12] R.Ronciani et al., Nucl.Phys. B529 (1998) 424
- [13] J.Dodd, S.McGrath, and J.Parsons, ATLAS Internal Note ATL-COM-PHYS-99-039 (1999)